

The Iris Recognition Based on Curvelet Transform and Improved SVM

Cheng-Xi Gu*, Cai-Dong Gu, Ya-Qin Li

Department of Computer Engineering, Suzhou Vocational University, Suzhou 215104, China

*Corresponding author, e-mail: chenxi_gugu@163.com

Abstract

In order to increase the accurate rates of the iris recognition, this paper proposes iris recognition method based on the combination of second generation curvelet transform and the Support Vector Machine Category correction. The images collected from iris image acquisition system are identified. First, rotation correction of iris and spot removal are carried out for collecting iris images. Then, iris images are through rectangular conversion, filter to extract edge point element from which judge the iris image quality. Furthermore, LoG operator is adopted to extract high-frequency energy on both sides of the iris pupil local area, and special judgment is taken out for pupil blocking by eyelids, eyelashes on basis of the energy spectrum. Finally, the cuckoo search algorithm is designed to optimize iris classifier of SVM parameters, and with the second generation curvelet transform algorithm, to complete iris recognition Results show that iris recognition with the CASIA 1.0 database, which contains 756 images of 108 eyes, is an efficient method for iris recognition with high recognition accuracy of iris image.

Keywords: the second curvelet transform, support vector machine, characteristics extraction

Copyright © 2014 Institute of Advanced Engineering and Science. All rights reserved.

1. Introduction

The iris recognition has been a wide concern that relates to machine learning, image processing, psychology and knowledge of other disciplines. In recent years, as an important part of biometric, iris has many characters such as unique, can be collected, difficult to change and non-invasive. Iris recognition has been widely used in national security and information security [1].

Iris recognition is a pattern classification problem, including iris feature extraction and classifier construction. There are several methods for Iris feature extraction: 2D Gabor filtering algorithm, Wavelet zero crossing detection algorithm, Laplacian pyramid algorithm, and 2D Haar wavelet transform algorithm. These feature extraction algorithm can only express singularity of points in iris image, but cannot extract the singularity characteristics of image curve [2, 3].

This paper presents a based on the combination of second generation curvelet transform and the Support Vector Machine Category correction. Curvelet transform algorithm is a new multi-scale image geometric analysis tool that can better extract the singularity characteristics of the iris image. The classifier constructed mainly includes the distance and artificial intelligence algorithms, distance algorithm mainly includes the Hamming distance and Euclidean distance, and artificial intelligence algorithms include artificial neural networks and support vector machine (SVM). Distance algorithm is simple and easy to achieve, but it is a linear classification algorithm with low iris classification accuracy. The artificial neural network is a machine learning algorithm based on structural risk minimization with nonlinear classification ability, but the network structure is complex and prone to over-fitting. SVM specifically for the small sample, high-dimensional, nonlinear classification problems, is a better way to solve over-fitting problem of neural network. With excellent generalization ability, it becomes the best iris recognition classifier. However, in the application, it also has the problem of parameters optimization [4-6]. Some researchers present particle swarm optimization, genetic algorithm to select SVM parameter, but the presence of local optima and other defects of these algorithms affect the accuracy of iris recognition.

The structure of the paper is as follows. First, rotation correction of iris and spot removal are carried out for collected iris images. Then, iris images are through rectangular conversion, filter to extract edge point element from which judge the iris image quality. Furthermore, LoG

operator is adopted to extract high-frequency energy on both sides of the iris pupil local area, and special judgment is taken out for pupil blocking by eyelids, eyelashes on basis of the energy spectrum. Finally, the cuckoo search algorithm is designed to optimize iris classifier of SVM parameters, and with the second generation curvelet transform algorithm, to complete iris recognition Results show that the proposed algorithm is an efficient method for iris recognition with high recognition accuracy of iris image [7-10].

2. The Second Generation of Curvelet Transform

The first generation of Curvelet transform needs several steps-sub-band composition, block smooth, regularization and Ridgelet transformation. The implement is complex and the data redundancy is quite large. Candès, Donoho and etc. propose the second generation Curvelet transform based on the Curvelet transform without the need of Ridgelet transform. It greatly reduces the data redundancy and the computation speed is rapid [11, 12].

Definition 1: Assume in two-dimension space, there are smooth, non-negative radial window $w(r)$ and angle window $V(t)$, they meet the admissibility conditions as follows:

$$\begin{cases} \sum_{j=-\infty}^{\infty} w^2(2^j r) = 1 & r \in (3/4, 3/2) \\ \sum_{j=-\infty}^{\infty} V^2(t-l) = 1 & l \in (-1/2, 1/2) \end{cases} \tag{1}$$

For all scales $j \geq j_0$, the Frequency window of the Fourier frequency domain is defined as:

$$U_j(r, \theta) = 2^{-3j/4} W(2^{-j} r) V\left(\frac{2 \lfloor j/2 \rfloor \theta}{2\pi}\right) \tag{2}$$

In the equation, $\lfloor j/2 \rfloor$ represents the integer part of $j/2$.

U_j is a kind of wedge window in polar coordinates as shown in Figure 2. The shadow part is the wedge window which is the supportive interregional of Curvelet [13-15].

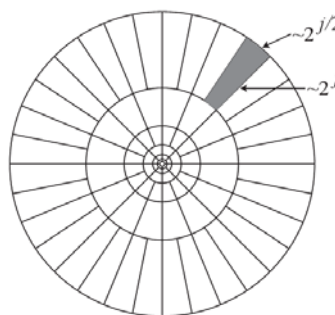


Figure 1. The Frequency Segments of the Continuous Curvelet Transforms

Definition 2: The Curvelet transform scale parameter is 2^{-j} , the rotation angle sequence is $\theta_{j,l} = 2\pi \times 2^{-\lfloor j/2 \rfloor} \times l$, displacement parameters series is $x_k^{(j,l)} = R_{\theta_{j,l}}^{-1} (k_1 2^{-j}, k_2 2^{-\lfloor j/2 \rfloor})^T$. The second generation Curvelet is defined as:

$$\varphi_{j,l,k}(x) = \varphi_j [R_{\theta_{j,k}}(x - x_k^{(j,l)})] \quad (3)$$

In the equation, $R_{\theta_{j,l}}$ is the rotation angle, $\theta_{j,l}$ is the rotation matrix.

Definition 3: The continuous Curvelet transform in frequency domain is:

$$\begin{aligned} c(j,l,k) &= \frac{1}{(2\pi)^2} \int \widehat{f}(\omega) \widehat{\varphi}_{j,l,k}(\omega) d\omega = \\ &= \frac{1}{(2\pi)^2} \int \widehat{f}(\omega) U_j(R_{\theta_{j,l}} \omega) \exp[i \langle x_k^{(j,l)}, \omega \rangle] d\omega \end{aligned} \quad (4)$$

Real value, non-negative and low-pass window W_0 is introduced and it meets:

$$|W_0(r)|^2 + \sum_{j \geq 0} |W(2^{-j}r)|^2 = 1 \quad (5)$$

For $k_1, k_2 \in Z$, the Curvelet in coarse scale can be defined as:

$$\begin{cases} \varphi_{j_0,k}(x) = \varphi_{j_0}(x - 2^{-j_0}k) \\ \widehat{\varphi}_{j_0,k}(\omega) = 2^{-j_0} W_0(2^{-j_0}|\omega|) \end{cases} \quad (6)$$

Curvelet can decompose the information to two parts- coarse scale and fine scale [16-18]. The Curvelet transform is consisted of the direction element $(\varphi_{j,l,k})_{j \geq j_0, l, k}$ in fine scale and isotropic wavelet $(\varphi_{j_0,k})_k$ in coarse scale. When applies Curvelet transform algorithm to iris characteristics extraction, the discrete form should be used. The transformed frequency segments are shown as Figure 2.

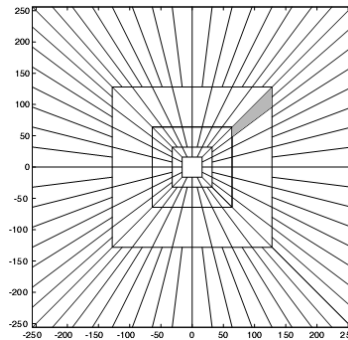


Figure 2. The Frequency Segments of Discrete Curvelet Transforms

3. Iris Feature Extraction

3.1. Removal of the Pupil Spot and Iris Rotation Correction Partitioning

Auxiliary light source of image acquisition equipment usually causes flare in the pupil, and method in this paper is based on region growing spot treatment.

Normalized iris image translation should be adjusted before feature extraction. Adjustment algorithm can be divided into three steps:

Step 1: With lower left corner of the normalized iris image as the origin of coordinates to establish left-handed coordinate system. Through the ellipse fitting method, register and log in the intersection of x-axis and the image, B and B1, and calculate level-shifted amount of the two images $\Delta x = x_{B1} - x_B$.

Step 2: according to Δx to construct translation operator (7)

$$\begin{cases} x' = x + \Delta x + \lambda \\ y' = y \end{cases} \quad (7)$$

That means, when the value of y is unchanged, the image logged in will level-shift $\Delta x + \lambda$ bits wherein λ represents the fitting correction operator. Large amount of experiments show that $\lambda = 3$ is the best algorithm performance obtained by the proposed algorithm.

Step 3: Adjust the error identification caused by rotation.

Traversing two entropy arrays to extract the interesting region and sub-block number, and generate the identify square for sub-block corresponding to close entropy. The size of the generated identification matrix is different due to the quality difference of iris acquisition. But you can always find a matrix to meet identified needs, thus realizing adaptive feature of the algorithm. Figure 3 shows the whole process of a block matrix creation and recognition:

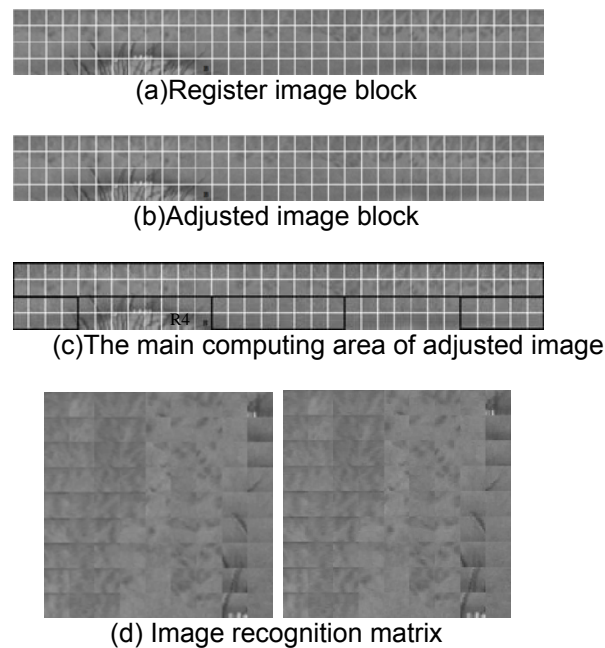


Figure 3. Processes of a Block Matrix Creation and Recognition

3.2. Rectangular Transformation for Iris Image

Assuming gray distribution of the input iris image is $I(x, y)$, after spot treatment, all gray value of the pupil is zero. $N(x)$ reflects the number of pixel points that gray value of each column is zero corresponding to x-coordinate; $N(y)$ reflects the number of pixel points that gray value of each row is zero corresponding to y-coordinate. Set the maximum point in $N(x)$ and $N(y)$ as the center, $R1$ smaller than radius of the pupil as the inner radius, $R2$ larger than outer radius of the iris as the outer radius. Iris image $I(x(\rho, \theta), y(\rho, \theta))$ in Cartesian coordinates annular is converted to rectangular image in polar coordinates $I(\rho, \theta)$. Conversion process is implemented by the following equation:

$$\begin{cases} x(\rho, \theta) = (1 - \rho) * x_p(\theta) + \rho * x_i(\theta) \\ y(\rho, \theta) = (1 - \rho) * y_p(\theta) + \rho * y_i(\theta) \end{cases} \quad (8)$$

Where in:

$$\begin{cases} x_p(\theta) = x_{p0}(\theta) + r_p * \cos(\theta) \\ y_p(\theta) = y_{p0}(\theta) + r_p * \sin(\theta) \end{cases} \quad (9)$$

$$\begin{cases} x_i(\theta) = x_{i0}(\theta) + r_i * \cos(\theta) \\ y_i(\theta) = y_{i0}(\theta) + r_i * \sin(\theta) \end{cases} \quad (10)$$

In the formula r_p and r_i are the inner and outer radius of the iris ring initially extracted. $x_p(\theta)$, $y_p(\theta)$, $x_i(\theta)$ and $y_i(\theta)$ are the coordinates on the inner and outer boundary of iris ring according to angle θ . Conversion is shown in Figure 4.

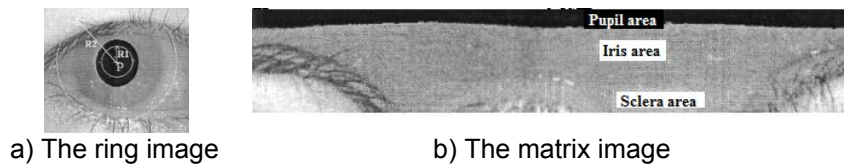


Figure 4. Schematic Polar Coordinate Conversions

3.3. Filtering Process

One-dimensional log-Gabor filter is not suitable for feature extraction of two-dimensional iris images, while 2D Log-Gabor extracts texture characteristic information from two directions—the radial and angular. So 2D Log-Gabor is the better

Gabor function is defined as:

$$g(x, y) = \frac{1}{2\pi\delta_x\delta_y} \exp\left[-\left(\frac{x^2}{\delta_x^2} + \frac{y^2}{\delta_y^2}\right)\right] \times \cos[2\pi f(x \cos \theta + y \sin \theta)] \quad (15)$$

In the formula, f is center frequency of the filter, θ indicates the direction of the filter and (δ_x, δ_y) represents the standard deviation of the Gaussian function.

Then the 2D Log-Gabor function can be described as:

$$h(x, y) = g(x', y') \exp[2\pi j(U_x + V_y)] \quad (16)$$

U and V are the two components of the center frequency along two axes.

In order to achieve coverage of multi directions, a plurality of filters must be constructed to form the multi-channel filter to express the difference between different textures. The iris feature extraction equation is:

$$F_{kj}(x, y) = H_{kj} \otimes I(x, y) \quad (17)$$

In the formula, $I(x, y)$ is the processed iris image, \otimes represents convolution operation, k indicates the k th scale and j indicates the j th direction.

It can be inferred from two-dimensional Log-Gabor filter results that after wavelet decomposition the results more intuitive and clearly reflect the trend of iris texture, and extract texture features conducive to iris recognition.

4. Judgment Quality of Iris Acquisition

4.1. Extract the High-frequency Energy of Iris Local Area

Defocused images have low pass filter characteristic, suppressing high frequency detail information of the original image so that the images become defocused. While the well focused images are rich in texture details and high-frequency energy, so you can extract the iris texture detail information to determine the degree of focus of the image. In addition, the richer the texture detail, the greater the high-frequency energy and the sharper the picture. Actually, the inevitable interference of eyelids and eyelashes to iris in collected iris image increases the high-frequency energy. If extract texture details from the entire iris area, it is easy to false positive defocused image into a clear image causing failure in iris recognition. To exclude the interference of eyelids and eyelashes to the iris region while reducing the complexity of the algorithm, we use the Laplacian of Gaussian (LoG) operator to extract the high-frequency energy of local iris area on both sides pupil due to there are seldom eyelids and eyelashes blocking except a few severe condition

Laplace operator is the second derivative of the image, with isotropic and displacement invariance to meet the different requirements of image edge sharpening. Suppose the pixel gray value of an image is $I(x, y)$, Laplace transform $L(x, y)$ is as follows:

$$L(x, y) = \frac{\partial^2 I}{\partial x^2} + \frac{\partial^2 I}{\partial y^2} \quad (11)$$

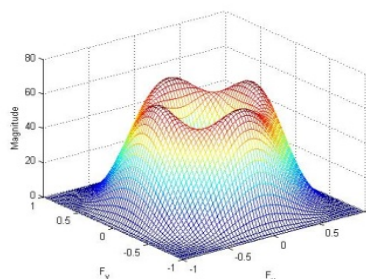
From which we can infer that it is sensitive to the noise. In order to decrease the sensitivity, the images are through Gaussian smoothing filter before the process with Laplace operator. This hybrid filter called Gaussian Laplacian filter. A two-dimensional LoG function with zero-crossing point center is shown as following:

$$LoG(x, y) = -\frac{1}{\pi\sigma^4} \left[1 - \frac{x^2 + y^2}{2\sigma^2} \right] e^{-\frac{x^2 + y^2}{2\sigma^2}} \quad (12)$$

Wherein σ is the Gaussian standard deviation.

-2	-4	-4	-4	-2
-4	0	8	0	-4
-4	8	24	8	-4
-4	0	8	0	-4
-2	-4	-4	-4	-2

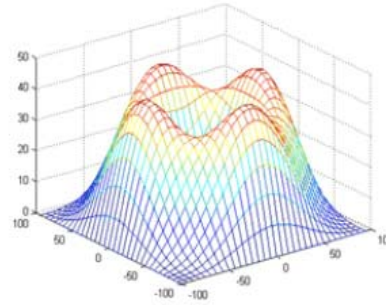
(a) Gaussian Laplace operator



(b) Fourier spectrum

Figure 5. Common LoG Operator and its Spectrum

-1	-1	-1	-1	-1	-1	-1	-1
-1	-1	-1	-1	-1	-1	-1	-1
-1	-1	+3	+3	+3	+3	-1	-1
-1	-1	+3	+3	+3	+3	-1	-1
-1	-1	+3	+3	+3	+3	-1	-1
-1	-1	+3	+3	+3	+3	-1	-1
-1	-1	-1	-1	-1	-1	-1	-1
-1	-1	-1	-1	-1	-1	-1	-1



(a) the convolution kernel of Daugman

(b) Fourier spectrum

Figure 6. The Convolution Kernel and Fourier Spectrum of Daugman

Because the image is a discrete set of pixels, we can only find a discrete convolution kernel approximates Gaussian Laplace operator. Commonly, different LoG operators can be got according to different σ set. This paper adopts the common 5*5 Gaussian Laplace operator (as shown in Figure 5). It is a convolution kernel with a band-pass filter, the center frequency of 0.5 and a bandwidth of 0.3750, while the classical 8x8 convolution kernel proposed by Daugman (shown as Figure 6) the center frequency of 0.28125 and a bandwidth of 0.1875. Therefore, the LoG discrete convolution kernel in this paper can select more high-frequency energy. In addition, Daugman method extracts frequency energy from the original image, while the proposed algorithm is from both sides of pupil region where concentrates iris texture, so the calculation speed of proposed algorithm is faster than that of Daugman's.

Convolution of LoG operator and R1, R2 separately is calculated and the energy can be obtained by formula (20)

$$f(R_i) = \frac{1}{W \times H} \sum_x \sum_y |C_i(x, y)| \quad (i = 1, 2) \quad (13)$$

$C(x, y)$ represents the convolution of (x, y) and Log operator, W and H are separately indicate the width and length of R1 and R2.

Then the sharpness evaluation indicators for the iris image to be evaluated I is:

$$f(I) = (f(R_1) + f(R_2)) / 2 \quad (14)$$

For the defocused blurred images, the detail information is lost and $f(I)$ is small, while for sharp image contours are clear and high-frequency energy and $f(I)$ are large. Therefore, it can be determined whether an image is defocused blurred by a threshold TH obtained from experiments: energy of images less than TH are blurred need to be abandoned and larger are sharp ones can do through the next step.

TH is defined as the mean of the greatest energy value of defocused blurred images and the least energy value of the sharp images in the training set.

$$TH = \frac{\max(f(I_1)) + \min(f(I_2))}{2} \quad (15)$$

I_1 is the defocused blurred images set and I_2 represents the sharp images set.

4.2. Eyelid Blocking Judgment

Because the gray value of eyelid is much larger than that of iris, average gray of rectangular R3 at the top of the pupil is selected for judging whether there is eyelid blocking. Then the images with severe blocking will be abandoned.

4.3. Eyelash Blocking Judgment

Comparing to iris images without eyelash blocking, we find the image with eyelash blocking contains large high-frequency components on the upper area of the pupil in the horizontal direction. Therefore, the blocking extent can be determined by extracting the horizontal frequency component of rectangular R3 above the pupil. This high-frequency information in this paper is described by gradient because the operator not only has good directivity, but also has a small amount of calculation.

The horizontal gradient of the rectangular region located above the pupil is G_x calculated as:

$$G_x(x, y) = I(x-1, y) - 2I(x, y) + I(x+1, y) \quad (16)$$

Take G , the mean of horizontal gradient, as the evaluation index.

$$G = \frac{1}{W \times H} \sum_x \sum_y |G_x(x, y)| \quad (17)$$

After the first two steps of the screening for multiple iris images captured, select the one in remaining horizontal images with smallest gradient for iris recognition.

5. Iris Recognition

5.1. Classification with Support Vector Machine

For a two-classification problem, there is data set (x_i, y_i) , $x_i \in R^n$, $y_i \in \{-1, 1\}$, $i = 1, 2, \dots, n$, x_i represents the classification attribute. In this paper, if the iris texture features should belong to the same iris. The output is $y_i = 1$, otherwise, $y_i = -1$. The Support Vector Machine optimal classification super surface is:

$$y = \omega \cdot \varphi(x) + b \quad (18)$$

In the equation, ω is the normal vector of the super surface, b is the offset vector of the super surface.

In order to maximize the distance between the vectors of the whole data in the training set and the optimal super surface, it can be transformed to quadratic optimization problem. That is:

$$\min J(w, \xi) = \frac{1}{2} \|w\|^2 + c \sum_{i=1}^n \xi_i \quad (19)$$

In the equation, c is penalty parameter which represents the penalty degree of the wrong samples.

The constrains for Equation (26) are:

$$\begin{cases} y_i(w \cdot \varphi(x_i) + b) \geq 1 - \xi_i \\ \xi_i \geq 0, i = 1, 2, \dots, n \end{cases} \quad (20)$$

In the equations, $\xi = (\xi_1, \dots, \xi_l)^T$.

The learning speed is slow while using the Support Vector Machine for classifying large amounts of samples. Lagrange multiplier can be introduced to transfer the problem to dual problem. The solving of the dual problem can speed up the classification. The classification function is:

$$f(x) = \text{sign} \left(\sum_{i=1}^n \alpha_i y_i (\varphi(x, x_i)) + b \right) \quad (21)$$

In the equation, sign is signed function, α_i is Lagrange multiplier.

For the linearly non-separable classification problems, the Support Vector Machine replaces the dot production function $\varphi(x, x_i)$ with the kernel function $K(x_i, x)$, therefore the final classification function of the Support Vector Machine is:

$$f(x) = \text{sgn} \left(\sum_{i=1}^n \alpha_i y_i k(x_i, x) + b \right) \quad (22)$$

5.2. The Iris Classifier SVM Parameter Optimization

- (1) The iris image data are collected and pre-processed.
- (2) The range of C and σ and the related parameters of the CS algorithm are configured.
- (3) Multiple nest positions are randomly generated and each nest position corresponds to a group of SVM parameters. The iris recognition precisions of each group of parameters are computed in order to find the optimal nest.
- (4) The optimal nest positions of the previous generation are kept. The positions of other nests are updated according to Levy flight in order to obtain a new group of nest positions and the recognition precisions of the nest are computed. The nest positions are updated based on the iris recognition precisions.
- (5) The nests with less discovered probabilities are kept and the nests with larger discovered probabilities are updated. The iris recognition precisions corresponding to the new nest positions are computed to replace those worse nest positions in order to obtain a new group of nest positions.
- (6) The optimal nest is found. The iris recognition precisions are evaluated to see whether it meets the practical requirement. If it meets the requirements, the searching stops and the optimal nest is outputted. Otherwise, return step (4) to keep searching.
- (7) The SVM parameters corresponding to the optimal nest positions are used to model and recognize the iris images.

6. Iris Recognition Experiment

6.1. Iris Database

The proposed iris recognition algorithm is applied to the iris recognition of the CASIA 1.0 database. The database contains 756 pictures of 108 eyes in which each eye has 7 pictures. They are divided to two stage collections. The first stage collects 3 pictures and the second stage collects 4 pictures. Parts of the samples in CASIA 1.0 are as shown in Figure 7.

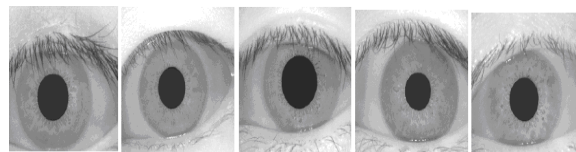


Figure 7. Iris Samples in the CASIA 1.0 Database

6.2. Performance Comparison

Under the same experimental conditions, two-dimensional Gabor filtering algorithm, wavelet zero crossing detection algorithm, Laplacian pyramid algorithm, and two-dimensional Haar wavelet transformation are used as comparison experiments. Their comparison results are as shown in Figure 8. The recognition errors of the second curvelet transform algorithm is the least and increases the recognition accurate rates relative to two-dimensional Gabor filtering algorithm, wavelet zero crossing detection algorithm, Laplacian pyramid algorithm, and two-dimensional Haar wavelet transformation. The comparison results illustrate the second curvelet transform algorithm can obtain more optimal iris characteristics and solve the iris characteristics extraction problem well.

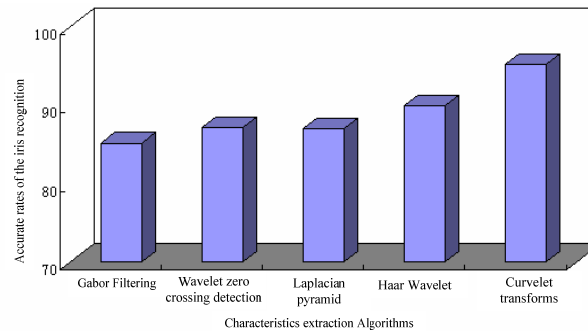


Figure 8 The Iris Recognition Accurate Rates Comparison

6.3. The Comparing with other SVM Algorithms

In order to verify the validity of the cuckoo searching algorithm for SVM parameter optimization, Particle swarm optimization algorithm and generic optimization algorithm of SVM are applied as the comparison experiment. The comparison results are shown in Figure 9. From Figure 11, the recognition accurate rate of the cuckoo searching algorithm is higher than particle swarm optimization algorithm and generic algorithm. The comparison results illustrate the cuckoo searching algorithm can find more optimal SVM parameters and solve the problem of SVM parameter optimization.

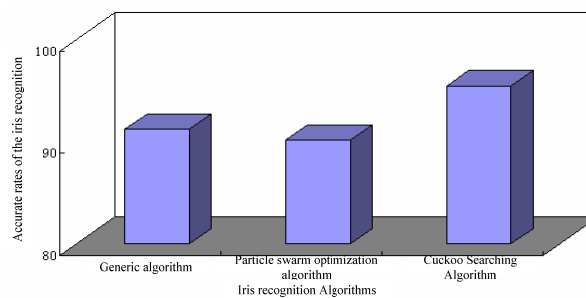


Figure 9. The Accurate Rates Comparison

7. Conclusion

In order to solve the problems in the current iris recognition characteristics extraction and classifier algorithm, this paper puts forward iris recognition model combining Curvelet transform algorithm and LSSVM in order to apply the advantages of the Curvelet transform algorithm and LSSVM. The simulation results verify the availability and superiority of the model which can be widely utilized in the identification area. With the increase of the application requirements, the random iris image contrast will be achieved in the future. Since the

uncontrollable factors in random iris image are great, how to effectively identify such images becomes a hot issue in next step. In addition, three-dimensional iris recognition will also become a topic aroused great concern.

References

- [1] Daugman JG. *Probing the uniqueness and randomness of iris codes: results from 200 billion iris pair comparisons*. Proc IEEE. 2006; 94(11): 1927-1935.
- [2] JG Daugman. High Confidence Visual Recognition of Persons by a Test of Statistical Independence. *IEEE Trans. Pattern Analysis and Machine Intelligence*. 2010; 15(11): 1148-1161.
- [3] JG Daugman. Statistical Richness of Visual Phase Information: Update on Recognizing Persons by Iris Patterns. *International Journal of Computer Vision*. 2001; 45(1): 25-38.
- [4] WC Chen. Nonlinear dynamics and chaos in a fractional-order financial system. *Chaos Solitons & Fractals*. 2008; 36(5): 1305–1314.
- [5] ZHANG Xiao-bing. Inverter Optimization Control Method Research and Simulation. *Computer Simulation*. 2011; 28(11): 409-412.
- [6] H Yoshito, O Makito, A Kazuyuki. Chaos in neurons and its application: Perspective of chaos engineering. *Chaos Solitons & Fractals*. 2012; 22(4): 305–314.
- [7] QL Li, PC Xu. Estimation of Lyapunov spectrum and model selection for a chaotic time series. *Applied Mathematical*. 2012; 36(12): 6090–6099.
- [8] Cao Jiajia, Jiang Dongfang, Wei Jingkui. A Medium Frequency Power Supply Design with Software Direct Digital Synthesized Variable Frequency. *Computer Measurement & Control*. 2012; 20(8): 2317-2323.
- [9] M Arash, A Majid. Developing a Local Least-Squares Support Vector Machines-Based Neuro-Fuzzy Model for Nonlinear and Chaotic Time Series Prediction. *IEEE Transactions on Neural Networks and Learning*. 2013; 24(2): 207–218.
- [10] E Kayacan, B Ulutas, O Kaynak. Grey system theory-based models in time series prediction. *Expert Systems with Applications*. 2010; 37(2): 1784–1789.
- [11] CL Lu, TS Lee, CC Chiu. Financial time series forecasting using independent component analysis and support vector regression. *Decision Support Systems*. 2009; 47(2): 115–125.
- [12] PP Balestrassi, E Popova, AP Paiva. Design of experiments on neural network's training for nonlinear time series forecasting. *Neurocomputing*. 2009; 72(4): 1160-1178.
- [13] QI Xiao-hui, WANG Feng, JIN Tao. Research on Multi-channel IF Sampling Digital down Conversion Application Technology. *Science Technology and Engineering*. 2013; 13(7): 1821-1826.
- [14] Z Chen, XS Liu, XD Zhuang. *A Fast Incremental Clustering Algorithm Based on Grid and Density*. Third International Conference on Natural Computation. 2010; 22(4): 1305–1314.
- [15] S Chandrakala, C Chandra Sekhar. *A Density based Method for Multivariate Time Series Clustering in Kernel Feature Space*. International Joint Conference on Neural Networks. 2008; 22(4): 1885-1890.
- [16] M Ester, HP Kriegel, J Sander. *A Density-Based Algorithm for Discovering Clusters in Large Spatial Databases with Noise*. Proc. of 2nd ACM SIGKDD Int'l Conf. on Knowledge and Data Mining. 2012; 22(4): 226–231.
- [17] S Aghabozorgi, MR Saybani, TY Wah. Incremental Clustering of Time-Series by Fuzzy Clustering. *Journal of Information Science and Engineering*. 2012; 28(4): 671-688.
- [18] Renoh C Johnson, Veena Paul, Naveen N, Padmagireesan SJ. Comparison of Curvelet Generation 1 and Curvelet Generation 2 Transforms for Retinal Image Analysis. *International Journal of Electrical and Computer Engineering*. 2013; 3(3): 366-371.